Late Archaean mantle metasomatism below eastern Indian craton: Evidence from trace elements, REE geochemistry and Sr–Nd–O isotope systematics of ultramafic dykes

A Roy[1*], A Sarkar[2], S Jeyakumar[3], S K Aggrawal[3], M Ebihara[4] and H Satoh[5]

[1]*Coal Wing, Geological Survey of India, DK-6, Sector-II, Salt Lake, Kolkata 700 091, India.*
[2]*Department of Geology and Geophysics, Indian Institute of Technology, Kharagpur, West Bengal 721 302, India.*
[3]*Fuel Chemistry Division, Bhaba Atomic Research Centre, Mumbai 400 085, India.*
[4]*Faculty of Science, Tokyo Metropolitan University, Tokyo 192-03, Japan.*
[5]*Geological Survey of Japan, Tsukuba 305-8567, Japan.*
[*]*e-mail: a_roy119@yahoo.com a_roy119@hotmail.com*

Trace, rare earth elements (REE), Rb-Sr, Sm-Nd and O isotope studies have been carried out on ultramafic (harzburgite and lherzolite) dykes belonging to the newer dolerite dyke swarms of eastern Indian craton. The dyke swarms were earlier considered to be the youngest mafic magmatic activity in this region having ages not older than middle to late Proterozoic. The study indicates that the ultramafic members of these swarms are in fact of late Archaean age (Rb-Sr isochron age 2613 ± 177 Ma, $Sr_i \sim 0.702 \pm 0.004$) which attests that out of all the cratonic blocks of India, eastern Indian craton experienced earliest stabilization event. Primitive mantle normalized trace element plots of these dykes display enrichment in large ion lithophile elements (LILE), pronounced Ba, Nb and Sr depletions but very high concentrations of Cr and Ni. Chondrite normalised REE plots exhibit light REE (LREE) enrichment with nearly flat heavy REE (HREE; $(\Sigma HREE)_N \sim 2$–3 times chondrite, $(Gd/Yb)_N \sim 1$). The $\varepsilon_{Nd}(t)$ values vary from +1.23 to −3.27 whereas $\delta^{18}O$ values vary from +3.16‰ to +5.29‰ (average +3.97‰ ± 0.75‰) which is lighter than the average mantle value. Isotopic, trace and REE data together indicate that during 2.6 Ga the nearly primitive mantle below the eastern Indian Craton was metasomatised by the fluid (± silicate melt) coming out from the subducting early crust resulting in LILE and LREE enriched, Nb depleted, variable ε_{Nd}, low $Sr_i(0.702)$ and low $\delta^{18}O$ bearing EMI type mantle. Magmatic blobs of this metasomatised mantle were subsequently emplaced in deeper levels of the granitic crust which possibly originated due to the same thermal pulse.

1. Introduction

Mafic dyke swarms are important for studying the extensional tectonics both in the continental and oceanic realm. They also provide valuable information regarding global geo-dynamic processes (Halls 1982). In particular, the ultramafic end members of mafic/ultramafic dyke swarms have been proved to be highly potential for understanding both mantle heterogeneity and its evolution (Zindler and Hart 1986 and references therein) and hence can be used to address some of the outstanding problems of Precambrian crust/mantle evolution as well. For example, a large number of trace element and isotopic (especially neodymium isotopic systematics) data suggest that most of the Archaean mafic crusts were derived from LREE-depleted sources (Hamilton *et al* 1983; Dupre *et al* 1984; Fletcher *et al* 1984; Huang *et al* 1986). Some evidences, however, exist which point out towards a

Keywords. Ultramafic dykes; Rb-Sr & Sm-Nd; source enrichment; eastern Indian craton.

Proc. Indian Acad. Sci. (Earth Planet. Sci.), **113**, No. 4, December 2004, pp. 649–665

complementary enriched mantle reservoir during the same time (De Paolo and Wasserburg 1979; Hegner *et al* 1984; Bowring *et al* 1989). Existence of these enriched components has been explained by models involving either plate tectonic processes whereby enriched mafic/ultramafic (Chase and Patchett 1988; Demney *et al* 2004; Spandler *et al* 2004) or alkali basalt (Galer and Goldstein 1991) crusts were either recycled back to the mantle or serial magmatism related to the hotspot type tectonics (Kroner and Layer 1992). Study of Archean ultramafic rocks (xenoliths, dykes etc.) is crucial in testing these models. As post crystallization deformation and metamorphism disturb pristine geochemistry and isotope systematics, it is desirable that such studies are made on undeformed ultramafic rocks that are either free from metamorphism or metamorphosed to a low grade only.

Most of the mafic dyke swarms of the Indian shield are of Proterozoic age. The oldest dyke dated so far is of early Proterozoic age (2420 Ma; Ikramuddin and Stueber 1976) occurring in southern Indian craton. It was considered that among all the other cratonic areas of India (viz., Aravalli, Bastar, Dharwar, eastern Indian craton etc.) the mafic dyke swarms in the eastern Indian craton are of much younger age (Devaraju 1995).

In this paper we report the occurrence of the oldest un-metamorphosed ultramafic dykes from the eastern Indian craton. The geochronology of the dykes is constrained by rubidium-strontium systematics. Additionally we report trace element, neodymium and oxygen isotopic data on these dykes and discuss their implications to the Archean mantle evolution. Petrography and major element data of these dykes have already been reported by Bose and Goles (1970) and Saha *et al* (1973).

2. Geology and sampling

The Eastern Indian Craton (EIC) (Singhbhum nucleus (Naqvi and Rogers 1987)) constitutes roughly a triangular shaped region with westward flanking Bastar Craton and bounded by Copper thrust belt in the north, Sukinda thrust in the south, relatively high grade metamorphic Satpura belt in the northwest and the eastern ghats granulite belt in the southwest. A major section of this craton is occupied by the Singhbhum granite batholithic complex of 3.2 Ga (Moorbath *et al* 1986) to 2.8 Ga (Saha 1994; figure 1) age, covering an area of about $10,000\,km^2$. It also contains numbers of shallow basins of different characteristics which are flanked by this granite batholith, viz., iron ore basins in the western sector containing enormous amount of iron ore deposits; Simlipal-Dhanjori basins dominated by volcanics and volcanoclastic sediments. Ancient rocks including the Older Metamorphic Group (OMG) of igneous and sedimentary rocks now metamorphosed to amphibolite facies, called as ortho-amphibolite and para-amphibolite respectively, and the Older Metamorphic Tonalite Gneisses (OMTG) occur as remnants within the batholithic complex. The OMTG intrudes synkinematically into the OMG amphibolites indicating that the later are oldest unit (3.3 Ga, Sharma *et al* 1994). This follows the Iron Ore Group (IOG) and it constitutes the major supracrustal unit in the Singhbhum-Orissa iron ore craton. These are made up of low grade metasediments including phyllites, tuffaceous shales, banded hematite jasper (BHJ) with iron-ore, ferrugeneous banded quartzite, local dolomite, acid-intermediate and mafic volcanics as well as mafic sill like intrusives. After the deposition of IOG, the crustal growth of this craton reached its peak with the vast intrusion of Singhbhum Granite batholith which occupies a major part of this craton. Subsequently a pause in crustal growth followed which was interrupted by a sedimentary (Singhbhum Group) and volcano-sedimentary cycles (Dalma, Simlipal, Dhanjori etc.) respectively and intrusions of gabbro-anorthosite along the eastern margin of Singhbhum granite batholith. It was followed by the deposition of the Kolhan Group of sediments. Finally the stabilization of this craton is attested by the intrusion of spectacular set of reticulating basic dyke swarms, known as Newer dolerite dyke (NDD) swarms, mainly confined in the southern part of Singhbhum shear zone.

Petrologically the NDD have been classified into three distinct groups namely, minor ultramafic/norites, dolerite/gabbro with micropegmatitic dolerites constituting about 99% of the dyke swarms and leucogranophyric dykes. All the three groups are considered to be genetically related representing cumulates, direct crystallization and partial melting products respectively (*op. cit.*). Published K-Ar dates, mostly on dolerites, give a long range from 2144 Ma to 950 Ma (Sarkar and Saha 1977; Mallik and Sarkar 1994) indicating them to be of definite Proterozoic age. No dates are, however, available either for the leucogranophyric or ultramafic dykes. In the outcrop NDD display mainly four distinct orientations viz., N-S, NNE-SSW, NNW-SSE and E-W among which NNE-SSW trend is the most dominant one. Samples for the present study are collected from two closely located NNE-SSW trending ultramafic dykes exposed at Keshargaria-Jatangpi area (figure 1). Based purely on the similarity of trend (NNE-SSW) with one set of NDD, these dykes which are intrusives within Singhbhum granite,

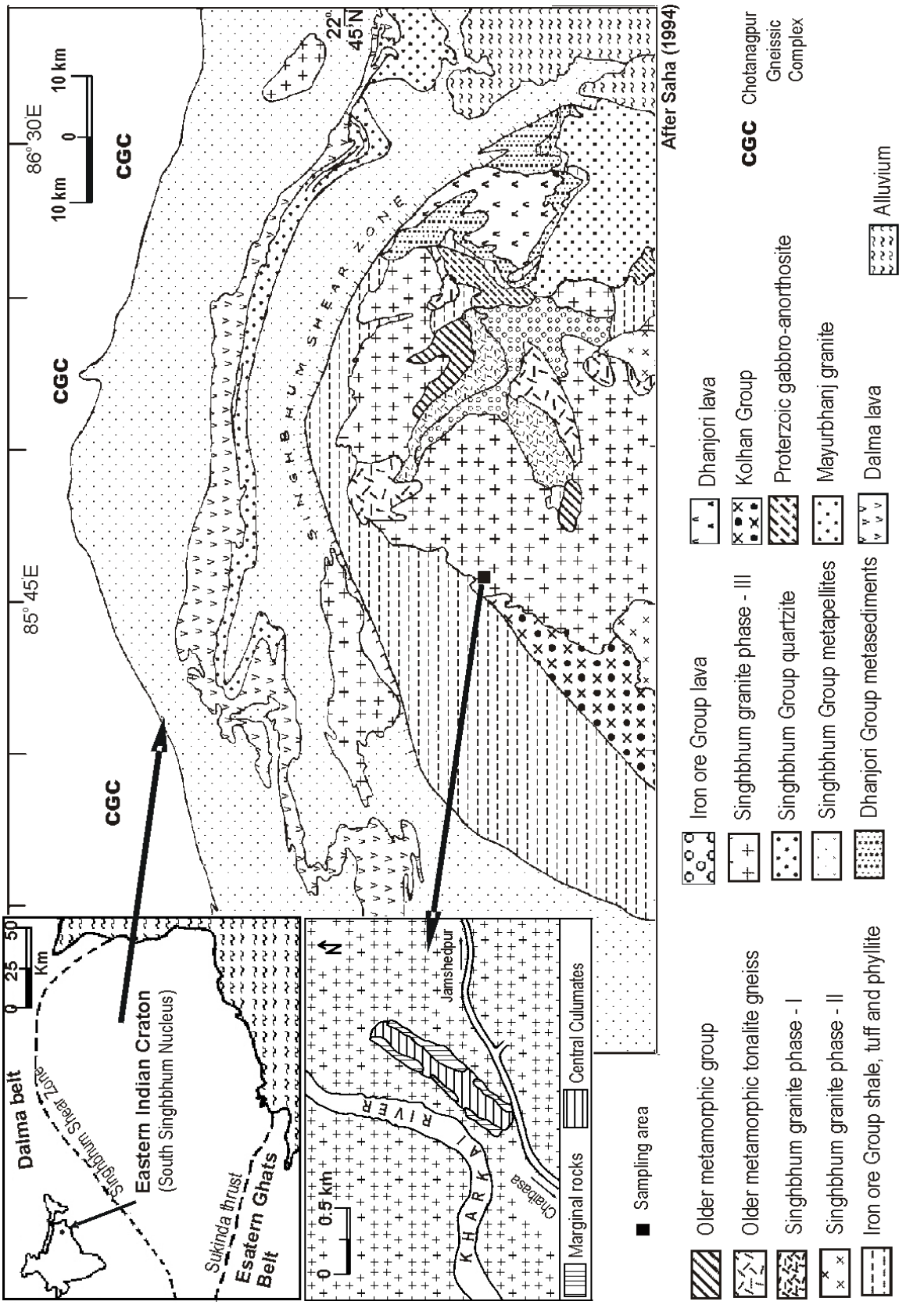

Figure 1. Geologic map of eastern Indian craton along with the detail geological map of ultramafic dyke from Keshargaria.

have been conventionally considered as ultramafic varieties of the mafic dyke swarms group (Saha 1994).

Detail petrography of these dykes are given in Bose and Goles (1970) and Saha *et al* (1973). However, we have also critically examined the petrography of the samples before carrying out geochemical and isotopic analyses. Petrographically, these dykes can be classified into two groups. One is harzburgite to pyroxenite (J-series) containing mainly cumulates of olivine and pyroxene (mostly enstatite) (figures 2A and 2C). Very few clinopyroxenes (mostly augite) are also present. Inclusions of opaque minerals (mostly magnetite and Cr-spinel) are present within both olivine and orthopyroxene. Modal mineralogy shows that the proportions of Olivine : Orthopyroxene : Clinopyroxene : opaque is 40 : 55 : 4 : 1. The other group (ND series) is of lherzolite type. The harzburgite type dyke has homogeneous texture having sharp contact with host granite whereas the lherzolite group has two varieties viz., a central coarse grained equant shaped olivine and prismatic pyroxene rich (with occasional presence of phlogopites) cumulate part and a marginal part with relatively fine grained rock containing hornblende, mica, quartz, feldspar but fewer olivine and pyroxene. Modal mineralogy of the central pure ultramafic part of this dyke shows that clinopyroxenes are more compared to the harzburgite one (figure 2B). Though olivines are to some extent altered, unaltered olivines are also present in considerable amount in both types of dykes. Like hurzburgite, opaque minerals (mostly magnetite and Cr-spinel) are also present within central lherzolite as accessory phases within both olivine and orthopyroxene. Modally central cumulates contain olivine : orthopyroxene : clinopyroxene : opaque $\sim$ 50 : 40 : 9 : 1. Presence of disequilibrium mineral assemblage like olivine, quartz, mica, etc. in the marginal samples (e.g., ND-28 & 29) indicates that possibly they represent mixing between original ultramafic magma with the host Singhbhum granite during emplacement.

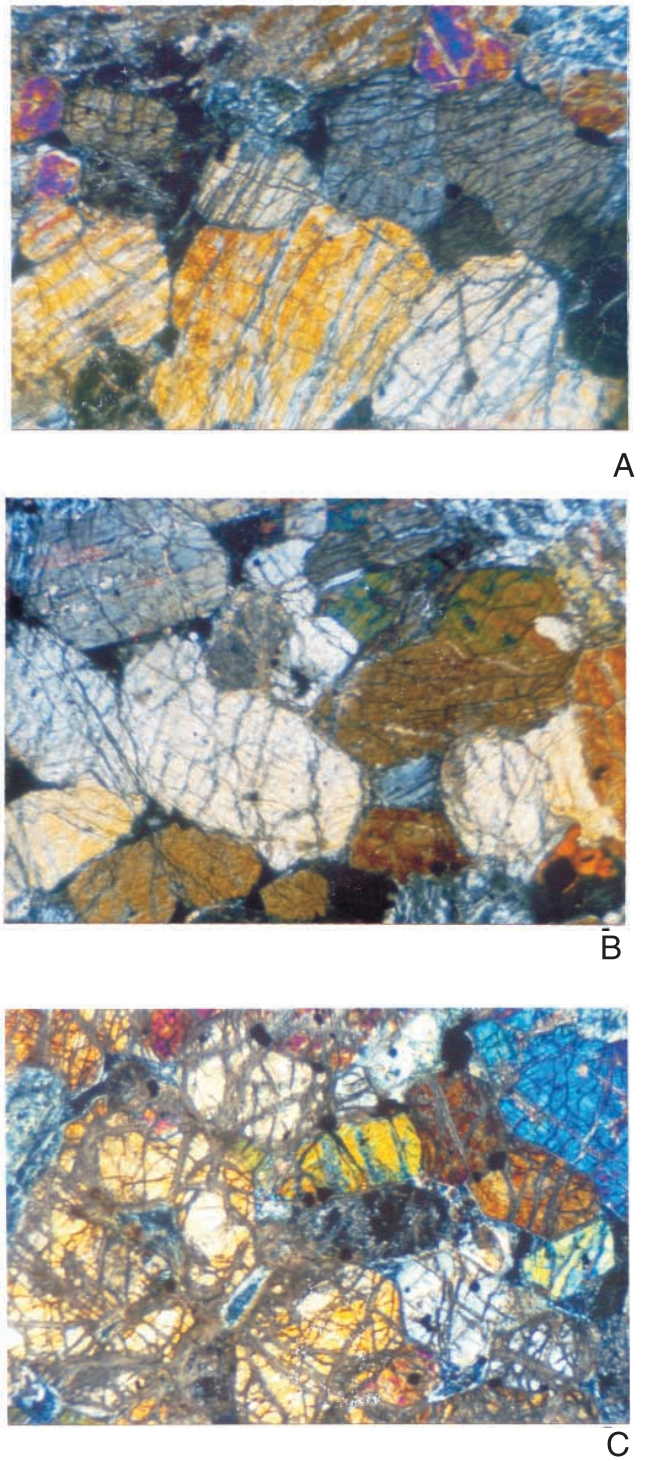

Figure 2. Photomicrographs of both hurzburgite and lherzolite dykes (under crossed nicols). **(A)** Cumulates of prismatic orthopyroxenes in hurburgite dyke; **(B)** Cumulates of prismatic orthopyroxenes and few clinopyroxenes in lherzolite dyke; **(C)** Cumulates of prismatic orthopyroxenes and equant shaped olivine in hurburgite dyke. Long dimension of each photograph is 10 mm.

3. Analytical techniques

Samples ($\sim$ 1 sq. cm. small chips) were powdered in tungsten carbide disc grinder. Care was taken to avoid inter-sample contamination by repeated washing of the grinder by de-ionized water and acetone. For isotopic analysis about 0.5 gm of powdered sample was taken and digested in a screwed TEFLON® vial following the method of Todland *et al* (1992). Typical sample digestion time was 3–4 days. Each sample solution was split into four aliquots, three of them were spiked with ^{84}Sr (80%), ^{145}Nd (80%) and ^{154}Sm (99%) for Isotope Dilution Mass-spectrometry (IDMS) and one

aliquot for isotopic composition of Sr and Nd. Sr and REE were separated from each aliquot by using DOWEX 50W- × 8 200–400 mesh cation exchange resin column (17 cm × 0.8 cm) in 2.5 N and 6 N HCl medium respectively (Sarkar *et al* 1996). Sm and Nd were subsequently separated from the bulk REE fraction following the modified method of Ramakumar *et al* (1980). The REE fraction was dried and taken into 90% CH_3OH + 10% 7.5 N HNO_3 medium and loaded onto BIO-RAD AG $1 \times 2 - 200$–400 mesh anion exchange resin column (4 cm × 0.4 cm). Sm and Nd were separated from this REE by eluting it with 90% CH_3OH + 10% 0.075 N HNO_3 medium. The elution scheme includes rejection of the first 2 column volumes followed by collection of Sm in the next 7 column volumes. Subsequent 11 column volumes were rejected and the Nd was collected in the final 12 column volumes. Pure Sr, Sm and Nd fractions were loaded on clean rhenium filaments in nitrate medium. All the analyses were carried out using a double filament assembly of MAT-261 thermal ionization mass-spectrometer at Bhaba Atomic Research Centre (BARC), Mumbai. Total procedural blanks for Sr, Sm and Nd are < 1 ng, < 200 pg and < 300 pg respectively. Reliability of IDMS was checked with basaltic standard BCR-1 which yielded concentrations of Sr, Sm and Nd as 332 ppm, 6.62 ppm and 28.82 ppm respectively and are in perfect agreement with the values reported by Lahaye *et al* (1995). Overall uncertainties in Sr, Sm and Nd concentration are $< 1\%$. Fractionation corrections for the Sr and Nd isotopic ratios for the unspiked samples were carried out with respect to $^{86}Sr/^{88}Sr = 0.1194$ and $^{146}Nd/^{144}Nd = 0.7219$ respectively. All quoted analytical errors are 2-sigma (2σ). Internal precision for $^{87}Sr/^{86}Sr$ isotopic ratios were monitored by running NBS-987 which gave 0.710226 ± 16 ($n = 22$). The internal precision for $^{143}Nd/^{144}Nd$ ratios were checked with both La Jolla and MERCK Nd standard which gave 0.511867 ± 08 ($n = 19$) and 0.511747 ± 06 ($n = 22$) values respectively. Reliability of the entire analytical procedure was checked by ion-chromatographic separation of Sr and Nd from BCR-1 rock standard and their mass spectrometric measurements. This provided $^{87}Sr/^{86}Sr$ and $^{143}Nd/^{144}Nd$ ratios of 0.704971 ± 23 and 0.512624 ± 18 and are in excellent agreement with the reported values viz., 0.704998 ± 15 and 0.512638 ± 11 respectively (Toyoda *et al* 1994).

Whole rock oxygen isotope analyses were carried out by Laser Fluorination (LF) technique at Tohoku University, Japan following a modified method of Sharp (1990). Powdered sample, kept in an Ni chamber, was pre-fluorinated (doubly distilled BrF_5) at room temperature and low vapour pressure to remove adsorbed H_2O on sample or chamber walls and was subsequently slow-heated by an RF-excited CO_2 laser in the ambient fluorine rich atmosphere. After laser heating the unreacted reagent was frozen into a cold trap. The evolved O_2 was converted to CO_2 over a hot carbon rod. The sample yield was measured by a pressure transducer and directly fed to the mass spectrometer inlet and measured. In all the samples, the yield was $> 95\%$. The analytical precision of oxygen data was monitored by LF analyses of NBS-28 quartz standard which yielded $\delta^{18}O$ value of 9.52‰ against recommended value of 9.66‰. In addition three more standards namely, JP-1 (a Geological Survey of Japan standard), San Carlos olivine and Ichinomegata olivine were also analysed which gave values like 5.38‰, 5.73‰ and 5.61‰ and are in good agreement with the recommended values of 5.35‰, 5.64‰ and 5.52‰ respectively. All $\delta^{18}O$ data have been reported with respect to SMOW.

Trace element analyses (including Rb) were carried out by ICP-MS at National Geophysical Research Institute, Hyderabad (Balaram *et al* 1996), whereas the REE were determined both by Instrumental Neutron Activation Analysis (INAA) at Tokyo Metropolitan University, Japan (for details see Roy *et al* 1997) and ICP-MS in NGRI, Hyderabad mainly to check the reliability of measured elemental concentrations. The analyses show that concentrations of REE are in good agreement between these two methods.

4. Results and discussion

Trace, REE, Sr, Nd and O isotopic data for these dykes are given in tables 1 and 2. Both the central cumulate portion of lherzolite dyke as well as harzburgite dyke have similar Ni (varying between 817 and 2205 ppm), Cr (4460–7034 ppm) and Co (99–142 ppm) concentrations. Only the marginal samples (ND 28 and ND 29) of lherzolite dyke contain much lower amount of Ni, Cr and Co consistent with the disequilibrium mineral assemblage as mentioned earlier indicating their mixed character. Concentration of large ion lithophile elements (LILE), particularly Rb and Ba, of both the dykes are also similar (5.15–19.88 ppm and 20–35.18 ppm) but are much less compared to the marginal samples of lherzolite dyke. High field strength elements (HFSE) like Nb, Hf , Zr, Y etc. in both hurzburgite and central part of lherzolite dykes are in much lower concentrations than those in marginal samples. Primitive mantle normalized (McDonough and Sun 1995) spidergram (figure 3a) for all the samples display a strong negative Nb anomaly but magnitude of the anomaly is considerably less in the marginal samples. Figure 3(a)

Table 1. *Trace and rare earth element concentrations of ultramafic dykes from eastern Indian craton.*

Sample no.	J 5	J 8	J 12	ND 15	ND 27	ND 28	ND 29	ND 30
Cr	5482	4465	4812	4483	6685	495	595	7034
Ni	1456	975	1475	817	1959	180	206	2205
Co	125.0	103.0	126.0	99.2	141.0	62.3	66.3	142.0
Sc	10.69	14.95	14.85	17.54	9.32	47.13	37.27	11.45
Zn	51.61	52.27	56.56	67.61	52.00	10.40	87.69	48.53
Rb	8.49	12.87	10.32	19.88	5.15	30.23	35.84	5.38
Cs	2.20	2.59	1.56	1.53	0.42	1.64	0.89	0.46
Ba	33.68	28.04	28.21	35.18	20.00	106.70	112.80	25.47
Sr	10.30	17.33	15.47	30.62	8.86	163.10	128.80	11.16
Nb	0.05	0.31	0.63	0.86	0.04	7.65	3.93	0.29
Hf	0.47	0.39	0.45	0.95	0.47	2.07	1.59	0.51
Zr	16.11	13.95	21.04	26.69	15.72	68.28	55.04	16.77
Y	3.73	3.54	5.49	6.08	3.38	24.13	18.39	3.93
Th	1.14	0.95	1.07	1.47	0.99	3.10	2.91	0.73
U	0.28	0.15	0.25	0.24	0.17	0.57	0.58	0.18
La	3.41	3.14	3.53	5.37	3.02	13.00	11.80	3.23
Ce	6.97	4.67	7.43	10.50	5.47	25.00	23.00	6.10
Pr	0.81	0.56	0.87	0.98	0.63	2.40	2.57	0.73
Nd	5.95	2.59	3.43	4.58	2.29	17.15	14.71	3.89
Sm	0.56	0.40	0.66	0.93	0.52	3.26	2.40	0.58
Eu	0.13	0.12	0.18	0.21	0.15	1.17	0.64	0.16
Gd	0.55	0.53	0.83	1.00	0.88	3.92	3.06	0.79
Tb	nd	0.11	nd	0.15	nd	0.69	0.49	0.23
Dy	0.38	0.35	0.98	1.00	0.41	2.40	1.78	0.32
Ho	0.10	0.10	0.25	0.26	0.14	1.04	0.71	0.15
Er	0.39	0.16	0.68	0.65	0.41	2.40	1.78	0.32
Tm	0.10	0.09	0.10	0.03	0.04	0.37	0.45	0.09
Yb	0.39	0.38	0.59	0.76	0.56	2.71	2.13	0.45
Lu	0.06	0.06	0.10	0.09	0.05	0.40	0.27	0.07
$(Gd/Yb)_N$	1.14	1.13	1.14	1.07	1.27	1.17	1.17	1.42
$(Ba/La)_N$	0.97	0.88	0.79	0.64	0.65	0.81	0.94	0.77
$(La/Sm)_N$	3.82	4.92	3.35	3.62	3.64	2.50	3.08	3.49

All concentrations are in ppm.
N = Chondrite normalized.

also shows pronounced negative Sr and Ba anomalies (again much less in marginal samples). Chondrite normalised REE pattern of these samples are shown in figure 3(b) exhibiting flat HREE pattern (with $\sim$ 2–3 times chondritic abundance, see Roy *et al* 1997) with only slight LREE enrichment. Both the central cumulate part of lherzolite and harzbugite dykes have similar REE patterns but their total REE (ΣREE) contents are lower than the marginal samples of Keshargaria. Interestingly, the host Singhbhum granites also display more or less similar REE pattern to these ultramafics (figure 3c) but with higher ΣREE content.

4.1 *Crustal contamination vs. source signature*

In general, the LREE enriched pattern with flat HREE ($(Gd/Yb)_N \sim 1$) and negative Nb anomaly (figures 3a and 3b), as seen in both the dykes can be produced by crustal contamination during the ascend of the magma (Polat *et al* 1997). However, ΣHREE $\sim$ only 2–3 times chondrites (Roy *et al* 1997), high Cr and Ni content, negative Ba, Sr anomaly and absence of pronounced Eu anomaly indicate an insignificant crustal contamination (Taylor and McLennan 1985). The similarity in REE and trace element patterns of marginal samples of the lherzolite dyke with those of central ultramafic rocks of both the dykes indicate that the marginal samples (ND 28 and ND 29), even if contaminated by the host Singhbhum granite during emplacement, still retain the pristine geochemical signatures. The effect of contamination of a pristine magma by the granitic country rock can be effectively assessed by Nb/La and Y/Zr ratios which change due to either mixing of different magmas or various degrees of partial melting of source or assimilation during emplacement. The ratio of these incompatible elements, however, remains mostly unchanged during the process of fractional crystallization (Ahmad and Tarney 1991 and references therein). Ideally an ultramafic

Table 2. *Rb-Sr and Sm-Nd concentrations and isotopic compositions and oxygen isotope values of the ultramafic dykes from eastern Indian craton.*

Sample no.	J 5	J 7	J 8	J 10	J 11	J 12	ND 24	ND 27	ND 28	ND 23	ND 15	ND 29	ND 30
Rb (ppm)	8.49	nd	12.87	nd	nd	10.32	nd	5.15	30.23	nd	19.88	35.84	5.38
Sr (ppm)	10.033	nd	17.329	nd	nd	15.474	nd	8.865	163.121	nd	30.624	128.821	11.164
$^{87}Rb/^{86}Sr$	2.468	nd	2.164	nd	nd	1.942	nd	1.69	0.537	nd	1.89	0.807	1.401
$^{87}Sr/^{86}Sr$	0.792071	nd	0.783202	nd	nd	0.776752	nd	0.768063	0.721410	nd	0.775552	0.731941	0.755152
	(16)		(18)			(12)		(28)	(21)		(18)	(17)	(21)
Sm (ppm)	0.622	0.469	0.498	0.671	0.572	0.748	0.576	0.569	3.637	3.729	1.013	2.669	0.625
Nd (ppm)	3.718	2.353	2.975	3.963	3.025	4.003	2.987	2.809	15.057	17.843	5.124	13.049	2.919
$^{147}Sm/^{144}Nd$	0.1012	0.1206	0.1075	0.1032	0.1142	0.1129	0.1166	0.1224	0.146	0.1263	0.1195	0.1237	0.1292
$f_{Sm/Nd}$	−0.486	−0.387	−0.453	−0.475	−0.419	−0.426	−0.407	−0.378	−0.258	−0.358	−0.392	−0.371	−0.343
$^{143}Nd/^{144}Nd^{\#}$	0.511068	0.511261	0.511172	0.511091	0.511111	0.511162	0.511190	0.511228	0.511812	0.511267	0.511209	0.511308	0.511435
	(10)	(08)	(09)	(16)	(10)	(12)	(09)	(17)	(09)	(12)	(09)	(11)	(11)
$\varepsilon_{Nd}(0)$	−30.63	−26.86	−28.6	−30.18	−29.79	−28.79	−28.25	−27.5	−16.11	−26.74	−27.88	−25.94	−23.47
$\varepsilon_{Nd}(T)$	1.23	−1.48	1.09	0.96	−2.32	−0.86	−1.57	−2.75	0.80	−3.27	−2.18	−1.62	−0.98
$T_{CHUR}(Ga)$	2.493	2.742	2.493	2.509	2.804	2.67	2.739	2.875	2.471	2.949	2.804	2.761	2.701
$\delta^{18}O(‰)$	3.16	–	4.4	–	–	3.72	–	3.24	5.29	–	4.58	3.95	3.39

nd = not determined.

$f_{Sm/Nd} = (^{147}Sm/^{144}Nd)_{Sample}/(^{147}Sm/^{144}Nd)_{CHUR}$ where CHUR is chondrite uniform reservoir having $^{147}Sm/^{144}Nd = 0.1967$.

$\varepsilon_{Nd}(0) = (\{(^{143}Nd/^{144}Nd)_{sample} - (^{143}Nd/^{144}Nd)_{CHUR}\}/(^{143}Nd/^{144}Nd)_{CHUR}) \times 10^4$, $(^{143}Nd/^{144}Nd)_{CHUR} = 0.512638$.

$\varepsilon_{Nd}(T) = \varepsilon_{Nd}(0) - 25.09 \cdot T \cdot f_{Sm/Nd}$.

$T_{CHUR}(Ga) = 1/\lambda \ln(1 + \{((^{143}Nd/^{144}Nd)_{sample} - (^{143}Nd/^{144}Nd)_{CHUR})/((^{147}Sm/^{144}Nd)_{Sample}/(^{147}Sm/^{144}Nd)_{CHUR})\})$.

Where λ = decay constant of $^{147}Sm = 0.654 \times 10^{-12}/a$.

$\delta^{18}O(‰) = (((^{18}O/^{16}O)_{sample} - (^{18}O/^{16}O)_{SMOW})/(^{18}O/^{16}O)_{SMOW}) \times 10^3$ SMOW = Standard mean ocean water.

error quoted within bracket are 2σ error − $\times 10^{-6}$.

magma having higher Nb/La ratio, if contaminated with the Singhbhum granite (of lower Nb/La ratio) should produce Nb/La ratio in between the original ultramafic magma and Singhbhum granite. All the samples, on the contrary, exhibit Nb/La ratios much lower, even lower than the bulk continental crust (Taylor and McLennan 1985). Moreover, in Zr-Y plot (figure 3), the Singhbhum granite shows lower Y/Zr (~ 0.1) ratio compared to these ultramafics (all having similar Y/Zr ratio ~ 0.38 including the marginal ones and close to N-MORB value, McDonough and Sun 1995). Figure 4 also shows strong correlation between these two variables for both marginal and other ultramafic samples ($r = 0.99$) indicating their cogenetic nature without much altering their pristine signatures during emplacement. This is also evident from similar Ni/Co and Cr/Ni ratios of these rocks (figure 5 and figure 6). We, therefore, believe that the geochemical signatures of these ultramafics essentially

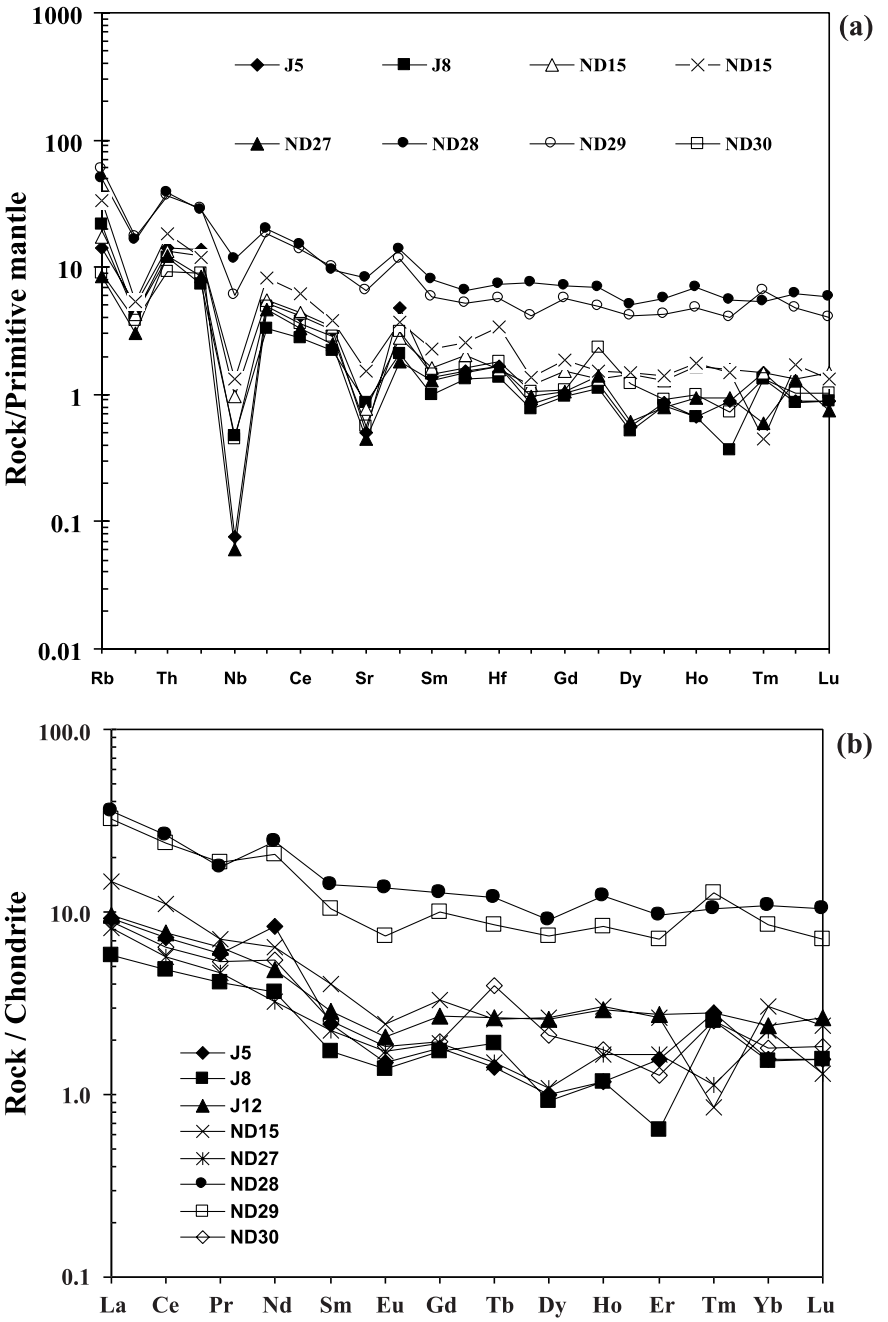

Figure 3. **(a)** Primitive mantle normalised trace element patterns of the ultramafics dykes. Note pronounced Ba, Nb and Sr anomalies (depletions). The marginal samples (ND 28, 29) have higher LILE contents but anomalies are less. **(b)** Chondrite normalised REE plot of ultramafics dykes. Note slight LREE enrichment and flat HREE pattern. Marginal samples have higher ΣREE. **(c)** Chondrite normalised REE plot of ultramafics dykes and Singhbhum granite (Saha 1994). Note similarity of pattern between granites and ultramafics.

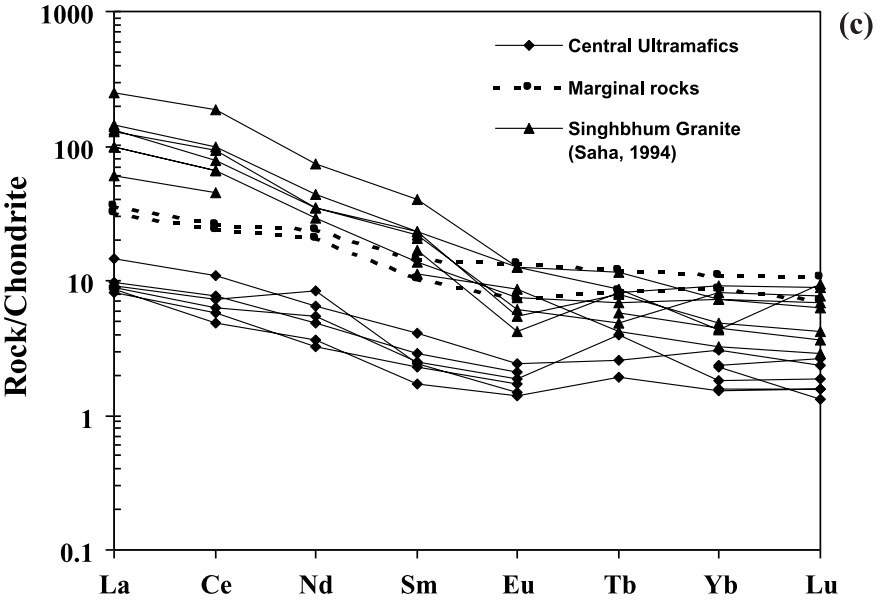

Figure 3. (*Continued*)

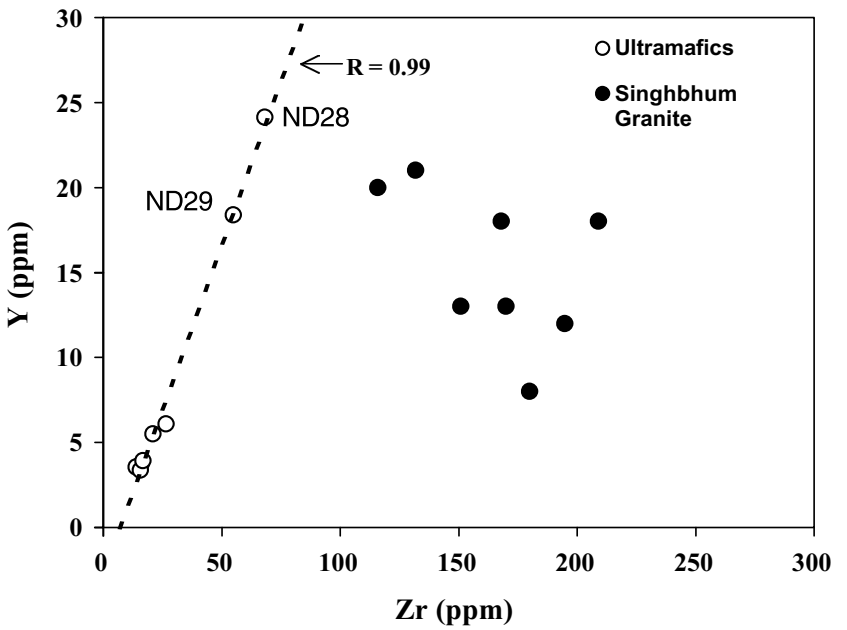

Figure 4. Zr-Y plot of the ultramafics and Singhbhum granite. Note similarity in Y/Zr ratio of the central ultramafics and marginal rocks showing high correlation ($R = 0.99$).

reflect characters of source material. This contention is further supported by Sr and O isotope data as discussed below.

4.2 *Sr isotopes*

Rb/Sr and $^{87}Sr/^{86}Sr$ ratios of the analysed dyke samples vary from 0.597 to 2.469 and 0.72141 to 0.79207 respectively. All the data are plotted on $^{87}Rb/^{86}Sr - ^{87}Sr/^{86}Sr$ plane in figure 7(a). The eight point whole rock isochron of these dykes yields an age of 2613 ± 177 Ma and initial Sr ratio (Sr_i) of 0.7020 ± 0.0044 (MSWD = 6). Figure 7(b) shows the 2.6 Ga reference isochron line along with the $^{87}Rb/^{86}Sr$ and $^{87}Sr/^{86}Sr$ ratios of Singhbhum granite phase-III (close to the locations of Keshargaria-Jatangpi; see Saha 1994 for definition) which clearly indicates that both the ratios of Singhbhum granite and central cumulates of the dykes are higher compared to the marginal samples. If at all crustal contamination perturbed the Rb-Sr systematics, the values of both $^{87}Rb/^{86}Sr$ and $^{87}Sr/^{86}Sr$ ratios of the marginal samples (ND28 and

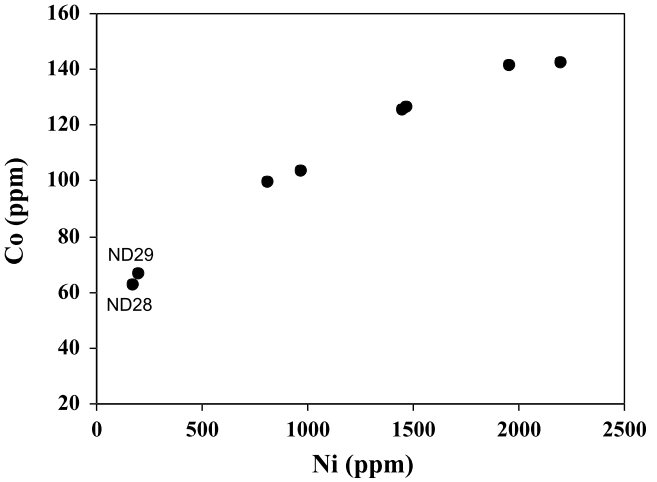

Figure 5. Ni-Co plot of the ultramafics.

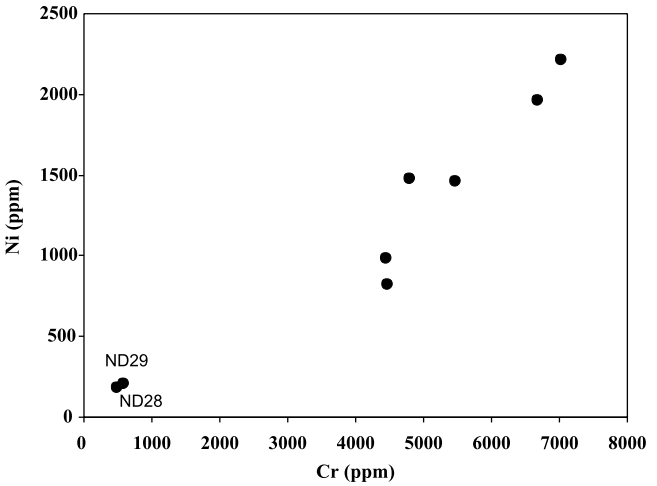

Figure 6. Cr-Ni plot of the ultramafics.

ND 29) would have been in between the central lherzolite and hurzburgite (devoid of crustal contamination) and host Singhbhum granite. But the figure 7(b) shows otherwise. Though petrographically the marginal samples (ND 28 and ND 29) are showing mixed character, they have much lower $^{87}Rb/^{86}Sr$ and $^{87}Sr/^{86}Sr$ ratios compared to the central dykes. This attests to the fact that these ultramafic rocks have retained their original signature (with respect to the Rb-Sr isotope systematics) even if they have been contaminated to some extent during emplacement. These observations along with the similar trace and REE patterns led us to argue that the isochron (figure 7a) is a real one and not fictitious. We, therefore, conclude that these dykes intruded the Singbhum granite around 2613 Ma i.e., during late Archaean time.

4.3 *Oxygen isotopes*

$\delta^{18}O_{SMOW}$ of the eight samples ranges from +3.16 to +5.29‰ (table 2), averaging +3.97 ± 0.75‰, which is lower than the calculated $\delta^{18}O$ values (+5.5 ± 0.4‰) of bulk composition of spinel-, garnet- and diamond-facies mantle (Mattey *et al* 1994). As the crustal contamination of an original magma tends to increase $\delta^{18}O$ values (Faure 1992), the lower $\delta^{18}O$ values of these ultramafics can not be due to crustal contamination. It is important to note that one of the marginal samples (ND-28, having a mixed petrography containing olivine, pyroxene, hornblende, mica, quartz and feldspar; see previous discussion) shows highest $\delta^{18}O$ value (+5.29‰), close to the general mantle composition. These observations together support our earlier contention (based on trace, REE and Sr isotope) that these rocks are not crustally contaminated but retained their pristine geochemical signatures. An alternative yet most plausible mechanism of low $\delta^{18}O$ values of the present ultramafics is interaction with hydrothermal fluid of lower $\delta^{18}O$ composition (Muehlenbachs *et al* 1974; Harmon and Hoefs 1995; Eiler *et al* 1996) either during post-crystallisation period or at source itself. Compilation of $\delta^{18}O$ values of hydrothermal fluid indeed indicates that they are low varying from −5 to −15‰ (Kyser 1986). Petrographic observation of these ultramafics show cumulates of olivine and pyroxene with insignificant (modally < 5%) serpentinisation (representative of a hydrothermal alteration product). Considering average modal proportion of Olivine : Orthopyroxene : Clinopyroxene : Serpentine as 60 : 30 : 5 : 5 in these rocks and its interaction with an average hydrothermal fluid of −10‰$\delta^{18}O$ composition, we calculate the final whole rock $\delta^{18}O$ value to be ∼ 4.8‰ (the respective mineral $\delta^{18}O$ values in mantle have been taken from Mattey *et al* 1994). This is not much different from the average mantle value and higher than the observed average $\delta^{18}O$ value of these ultramafics. The lowest $\delta^{18}O$ value of 3.16‰ (table 2) in fact requires interaction with an abnormally depleted fluid of ∼ −42‰ which is unrealistic. Additionally, the host Singhbhum granite also does not display any effect of hydrothermal alteration and retains unaltered mineralogy (Saha 1994). A post-emplacement hydrothermal interaction would also reduce the concentrations of most compatible elements like Ni, Cr and Co in the olivine and pyroxene as well as their respective correlations which are not observed in the present study (figures 5 and 6). During fractional crystallization, due to continuous removal of early mafic minerals from the magma, concentration of the compatible elements e.g., Ni, Cr and Co will gradually decrease in the remaining magma whereas $\delta^{18}O$ value will gradually increase. Hence, in an ideal case a negative correlation will be expected between $\delta^{18}O$ and either Ni or Cr or Co. If post crystallization hydrothermal alteration took place, this correlation would

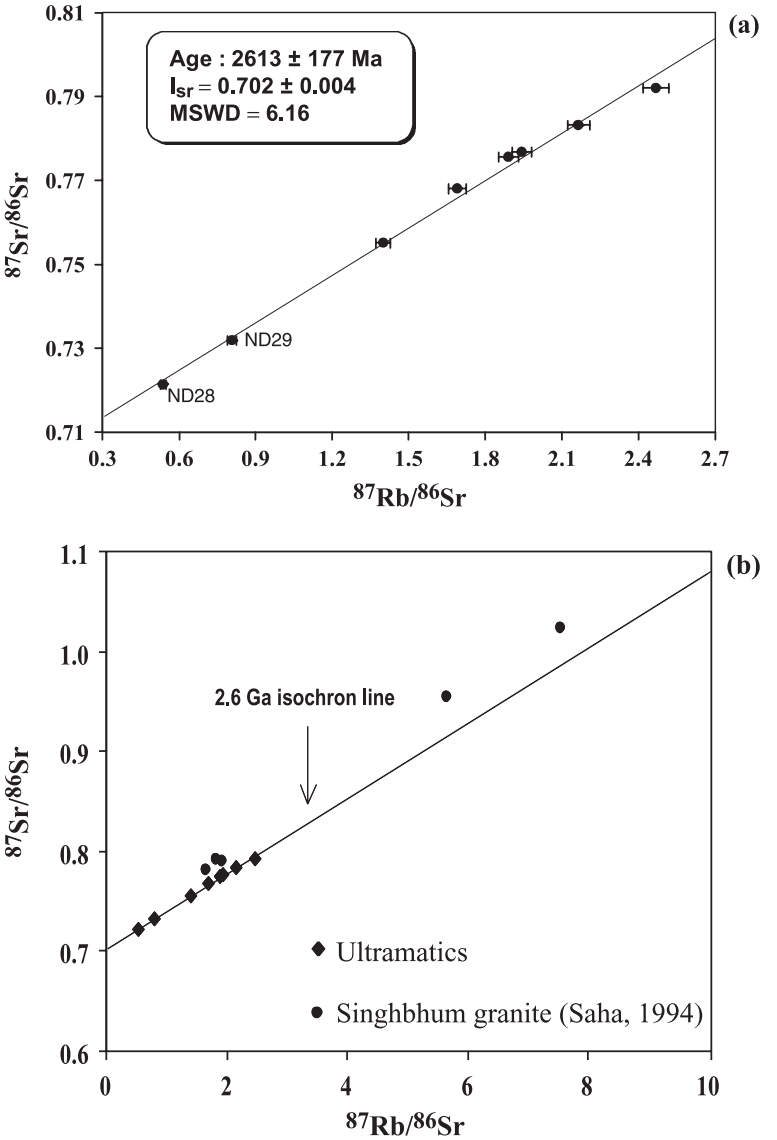

Figure 7. **(a)** $^{87}Rb/^{86}Sr$–$^{87}Sr/^{86}Sr$ whole rock isochron diagram of the ultramafics dykes. Only analytical errors have been considered for calculating the age (for details see text). The isochron is constructed using ISOPLOT program (model 3 solution; Ludwig 1988). **(b)** $^{87}Rb/^{86}Sr$–$^{87}Sr/^{86}Sr$ plot of the ultramafics and Singhbhum granite (phase III) along with 2.6 Ga reference isochron line. Note that the Singhbhum granites also lie close to the reference isochron but plotted towards higher Rb/Sr ratio side.

no longer exist. However, in the present study significant negative correlations are found between $\delta^{18}O$ with Ni, Cr and Co (figures 8, 9, 10) in these ultramafic samples. Therefore, this rules out any post-crystallisation hydrothermal fluid-rock interaction as the cause of these low $\delta^{18}O$ values and we conclude that the source of these rocks was itself depleted in oxygen isotopic composition. The most plausible mechanism of this source depletion may be the hydrothermal interaction and/or influxes of Fe-Ti-Cr rich melt (Zhang *et al* 2001) into the mantle itself. Compilation of LF $\delta^{18}O$ data on mantle minerals by Mattey *et al* (1994), however, indicates that the $\delta^{18}O$ values of olivine in hydrous and anhydrous lithologies are indistinguishable and the fluids, associated with exotic mantle oxygen isotope composition inherited from subducted oceanic crust, either lose its identity or the hydration process is a more localised phenomenon which involves fluids that are internally buffered. Our data do not reconcile with this explanation and instead indicates considerable influence of hydration at source. In fact, the low $\delta^{18}O$ values in some of the oceanic island basalt (OIB) have recently been explained by the involvement of altered and subducted oceanic crust during melting at mantle depths (Widom and Farquhar 2003; Demeny *et al* 2004). Not withstanding the difficulties in explaining the low $\delta^{18}O$ values of these ultramafics, the Nd isotope data also suggest a heterogeneous source

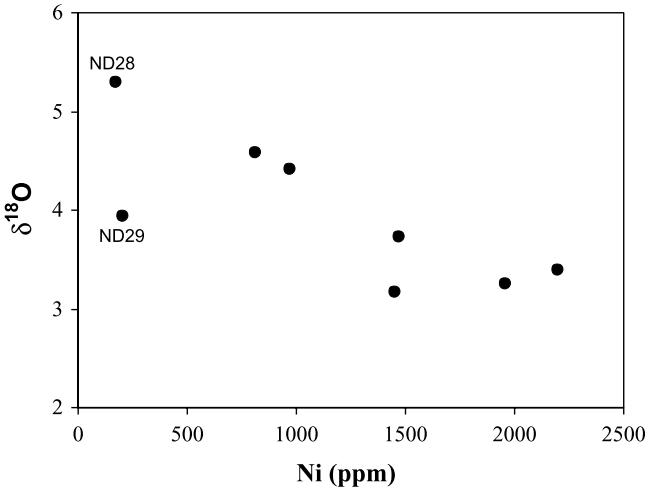

Figure 8. Ni-δ^{18}O plot of all ultramafics. Note the negative correlation.

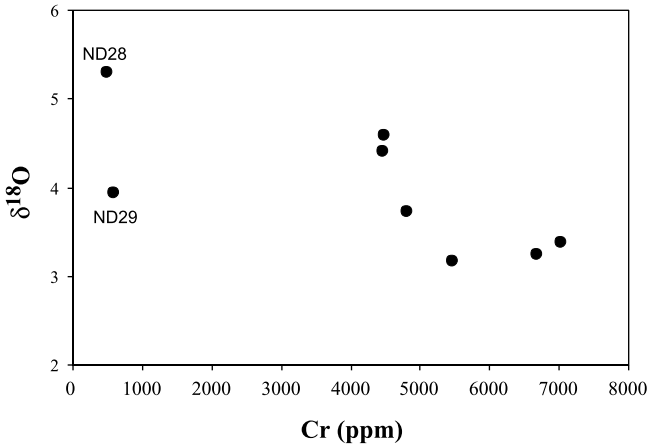

Figure 9. Cr-δ^{18}O plot of all ultramafics. Note the negative correlation.

best explained by mantle metasomatism caused by fluid from subducted crust as discussed below.

4.4 *Nd isotopes*

For all the 13 samples analysed, there is too little spread in $^{147}Sm/^{144}Nd$ (from 0.1012 to 0.1460; table 2) to construct an isochron. Compilation of partition coefficient (K_D) values show that the difference in K_D values between Rb and Sr is considerable during the process of crystallisation of ultramafic magma generated from a metasomatised mantle where clinopyroxene (mainly augite) is the suitable host for Sr (Halliday *et al* 1995 and Nielsen 1998). The rocks under the present study mostly contain olivine and orthopyroxene and slight variation in modal proportion of clinopyroxene can produce considerable spread in Rb/Sr ratio. In case of Sm and Nd this difference in K_D value is insignificant irrespective of the slight variation of modal percentage of clinopyroxene in

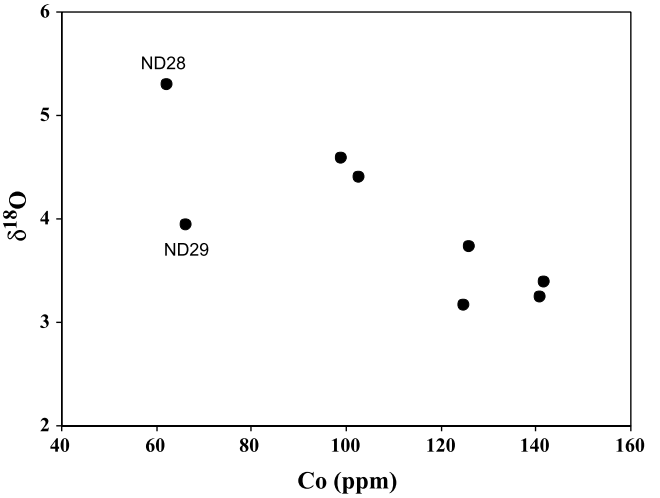

Figure 10. Co-δ^{18}O plot of all ultramafics. Note the negative correlation.

these ultramafic cumulates (*op. cit.*). Furthermore, if the source of the ultramafic magma is metasomatised (see the discussions above and below), the Rb and Sr contents will be more compared to the general primitive mantle as the metasomatised fluid is generally enriched in LILE whereas Sm and Nd contents remain mostly unaffected (Zindler and Jagoutz 1988). During the crystallization of this kind of ultramafic magma, some liquid may also be trapped either along the grain boundary or in between the grains (not possible to identify through petrographic means; Meen *et al* 1989) which will be enriched in Rb and Sr but depleted in Sm and Nd as Sm and Nd are generally stored within crystallising phases like olivine, orthopyroxene and clinopyroxene. Additionally, occasional presence of phlogopite in these ultramafic rocks also change Rb/Sr ratio whereas Sm/Nd is mostly unaffected. All these must have caused too little spread in $^{147}Sm/^{144}Nd$ values from 0.1012 to 0.1460 (table 2), to construct a meaningful isochron for these ultramafic rocks yet producing a reasonably good Rb-Sr isochron of 2613 Ma.

Also shown in table 2, ε_{Nd} (calculated back to 2.613 Ga) and T_{CHUR} (model ages using CHUR) values vary from +1.23 to −3.27 and 2.47 to 2.95 Ga (mean 2.69 ± 0.15 Ga) respectively. The ε_{Nd} values (positive and negative ε_{Nd}) indicate contribution from both enriched and depleted components at source i.e., a heterogeneous source with respect to LREE. LREE enrichment with low $^{143}Nd/^{144}Nd$ ratios of the samples (Blusztajn and Shimizu 1993) and absence of correlation in Nd-ε_{Nd} (2.6 Ga) plot (figure 11) also attest to the fact that this enrichment is not during crustal contamination or post crystallization alteration as mentioned earlier—rather source enrichment. Furthermore, the similarity of T_{CHUR} values (mean 2.69 Ga;

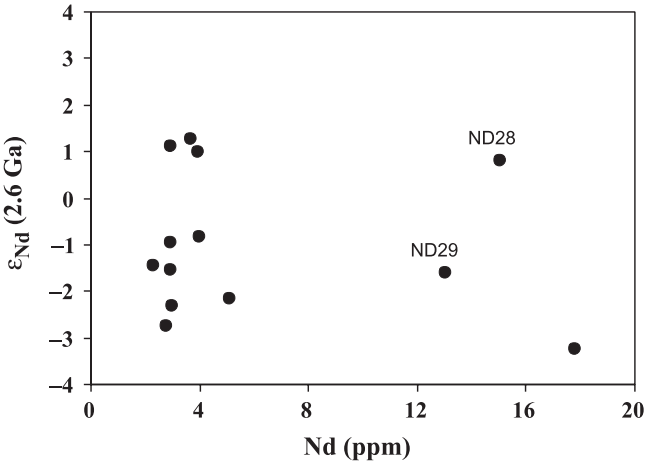

Figure 11. Nd-ε_{Nd} (2.6 Ga) plot of all ultramafics.

table 2) with the crystallization age (2.61 Ga) suggests that there is no significant time gap between the source-enrichment and the rock formation. Isotopically, therefore, the mantle below the eastern Indian craton had low $^{87}Sr/^{86}Sr$ ($\sim$ 0.702) and $^{143}Nd/^{144}Nd$ ratios (equivalent to EMI or enriched mantle I type proposed by Zindler and Hart 1986) along with variable ε_{Nd} values (with LREE enrichment) during the late Archaean time.

5. Implications

The variable ε_{Nd} during the late Archaean time below eastern Indian craton implies establishment of distinct isotopic reservoirs (both depleted and enriched). Global compilation of Nd isotopic data, obtained from basalts, ophiolite sequences and continental crustal materials, indicates three major mantle depletion peaks (increasing the volume of depleted mantle at the expense of primitive mantle) associated with three major peaks of crust building activities during the Precambrian viz., at 3.4 Ga, 2.7–2.6 Ga and 1.8–1.6 Ga (De Paolo 1981; Jacobsen and Wasserburg 1984; Bennett *et al* 1993; McCulloch and Bennett 1994). Interestingly, out of these, the most violent crust building peak during 2.7–2.6 Ga coincides with the intrusion age of eastern Indian craton ultramafic dykes. It is, however, difficult to find out the exact causative mechanism of the formation of enriched mantle reservoirs below EIC during late Archaean.

5.1 *Cause of source enrichment*

Three different processes can be visualised for such enrichment. These are deep seated plume magmatism, delamination of continental lithosphere and re-injection of enriched crustal reservoir via subduction (McKenzie and O'Nions 1983; Hawkesworth *et al* 1984; Weaver 1991; McCulloch 1993; McKenzie 1995; Hoffman 1997). Normally a deep seated plume originates from a depth within lower mantle to core-mantle boundary. Though definite subduction of Archaean crust started during 2.7 Ga (McCulloch and Bennett 1994), in an ambient steeper geothermal gradient (causing high magmatic activity but producing only thin buoyant crust; Bickle and Eriksson 1982; Arndt 1983; Nisbit and Fowler 1983; McCulloch 1993) with layered mantle convection (Allegre 1997) and faster plate movements, high angle subduction would be too difficult to operate. This, in turn, would reduce the chance of transport of enriched component deep into the mantle and thereby initiation of plume activity (McCulloch 1993). Moreover, it is difficult to visualize a plume related mechanism that can cause selective depletion of some incompatible elements like Ba and HFSE like Nb but preserving a primitive mantle-like ΣHREE concentration. Delamination of the denser lower crust, on the other hand, requires existence of considerably thicker and compositionally variable (differentiated) crust (Rudnick 1995). During pre-2.7 Ga period crust building activity was not too high, also the geothermal gradient was too high to produce thicker-differentiated crust. Also delamination of the lower continental crust cannot significantly reduce the Nb/La ratio of the upper mantle compared to the bulk continental crust (Taylor and McLennan 1985). These, along with low Sr_i ($\sim$ 0.702), ΣHREE $\sim$ 2–3 times chondrite of eastern Indian craton ultramafics rule out the possibility of both delamination or plume magmatism as a cause of enrichment of lithospheric mantle below the eastern Indian craton. We, therefore, postulate that the subduction induced mantle metasomatism was the only process by which the mantle below the eastern Indian craton could be enriched producing heterogeneous ε_{Nd}, low $\delta^{18}O$ and Ba, Nb depletions. It is possible that due to the subduction of the earlier (pre-2.6 Ga) oceanic (mafic) crust, fluid ($\pm$ silicate melt) was squeezed out from the slab and incorporated into the overlying mantle wedge. As this fluid generally contains H_2O, CO_2 and chloride ions, it will be enriched in moderately strong acids like Rb, Ba and Sr whereas depleted in very strong acid like Nb (Keppler 1996). Among Rb, Ba and Sr, Rb is of least acidic character. Furthermore, solubility and mobility of Rb in chloride medium is higher compared to Ba and Sr (*op. cit.*). This could explain the relative depletion of Ba and Sr compared to Rb. However, Ba depletion has also been reported to be either due to the presence of Ba-depleted sediment subduction-component at source (Smith *et al* 1996) or crustal recycling into the mantle (Nielsen *et al* 2002). We, therefore, consider that the metsomatic

interaction at source between fluids coming out of subducted slab and mantle was the main cause of LREE (and LILE) enrichment and Nb (HFSE) depletion. Since the mobility of Rb and Sr in the melt (*in situ* silicate)-fluid phase ($H_2O + CO_2$ and chloride medium) interaction is considerably higher than Sm and Nd (LREE), the fluid induced melt in the upper mantle wedge becomes isotopically more homogeneous with respect to Rb-Sr compared to Sm-Nd, causing variable ε_{Nd} ($\sim +1.26$ to -3.24) values. The lower $\delta^{18}O$ values of these ultramafics compared to the average mantle (table 2) also, in all likelihood, point towards the subduction related hydrothermal water/fluid and/or Fe-Ti-Cr rich melt invasion at the source (Zhang *et al* 2001; Demeny *et al* 2004).

Global compilation of ε_{Nd} data of mafic-ultramafic rocks exhibits, in addition to a strong depletion peak, significant presence of enriched mantle component around 2.7–2.6 Ga (McCulloch and Bennett 1994). Theoretical model calculation shows that along with vigorous crust building activities the subduction (low angle?) was also initiated during the same time (*op. cit*). It is tempting to speculate that a majority of these source enrichments were caused by this subduction induced mantle metasomatism (Spandler *et al* 2004 and references therein) as found in the ultramafic dykes of eastern Indian craton.

5.2 *Dyke age and cratonic stabilization*

It is important to mention that the late Archaean age of 2.6 Ga of Keshargaria-Jatangpi dykes indicates that the NDD swarm has much longer temporal range from 2.6 Ga to 0.95 Ga (with episodic intrusive activity cf. 2.6 Ga, 2.1 Ga, 1.5 Ga, 1.1 Ga; this work; Saha 1994; Mallik and Sarkar 1994) and is definitely not the youngest mafic magmatic activity as thought by earlier workers. Alternatively, these different episodes may imply emplacement of genetically unrelated dyke suites and hence grouping them purely on the basis of structural trends may not be justifiable. Finally, a close look at the emplacement age of the older dyke swarms from other cratonic blocks of India viz., Bastar, south Indian craton etc. reveals an interesting feature. The oldest mafic dyke activities in south Indian craton viz. Kolar gold field and other parts of Mysore have been dated to be $\sim$ 2.4 Ga (Ikramuddin and Stueber 1976; Sarkar and Mallik 1995). Mafic dykes within Bundelkhand granite are not older than 1.8 Ga (Sarkar 1997). Dolerite dyke swarms from adjacent Bastar craton are also of mid-Proterozoic age (1.2 Ga; Sarkar *et al* 1990). Since emplacement of dyke swarms are causally related to the stabilisation of cratons (Halls 1987), the 2.6 Ga emplacement age of eastern Indian craton ultramafic dykes suggests that among all cratonic blocks of Indian shield, the eastern Indian craton possibly experienced earliest stabilisation event. The youngest phase (III) of the Singhbhum granite batholithic complex, within which the ultramafic dykes were emplaced, possibly represents the end of the major crust building activity in eastern Indian craton.

5.3 *Mode of dyke emplacement*

Tectonically emplaced peridotitic rocks of either alpine type or ophiolite type within granitic country rocks have been reported from various localities world over where subsequent serpentinization might have eased further movement towards the shallower crustal level (Galan and Duthon 1996; Hall 1996). In addition intrusive peridotite bodies have also been reported from different places e.g., Lherz, Mount Albert, etc. (Loomis 1972; MacGregor and Basu 1979; Jahn *et al* 1999). Identifying the exact mode of emplacement of these bodies is often problematic as the contact relationships are frequently obscured by the serpentinization and faulting. Detail studies of some of these bodies indicate emplacement both as a solid hot body (resulting in contact metamorphosed aurioles) or molten magma (producing a mixed contact rock; Hall 1996). This leads to two possible interpretations:

- the peridotite originated at much greater depth or
- the magmatic events leading to the crystallization of the peridotite did not pre-date its eventual emplacement.

Cumulates of the ultramafic bodies of Keshargaria-Jatangpi indicate that they were crystallised from the magma in equilibrium condition. Moreover, the youngest phase (III) of the Singhbhum granite from nearby locations (e.g., Juldhia and Jorapokhar) of these dykes yielded Rb-Sr ages like 2860 ± 250 Ma and 2880 ± 259 Ma respectively (Saha 1994), which are close to Rb-Sr ages of the ultramafic dykes within error. This indicates that the same thermal pulse might have been responsible to produce the mafic/ultramafic magma from the partial melting of metasomatised mantle and extensive late Archaean granite intrusion. Possibly during the emplacement and final stabilisation event of the Singhbhum granite numerous magma blobs were generated due to the melting of overlying metasomatised mantle. These might have slowly cooled down within the Singhbhum granite at a relatively deeper level resulting in equilibrium cumulate texture represented by the Keshargaria-Jatangpi ultramafics. Interestingly these more

evolved members of NDD also have much younger ages (varying from 2.1 Ga to 0.9 Ga; Sarkar and Saha 1977; Mallik and Sarkar 1994). More detailed geochronological and geochemical studies of all varieties of NDD are required to fully understand the emplacement of this spectacular dyke swarm both in time and space.

6. Conclusions

- The intrusion age of the ultramafic dykes from Keshargaria-Jatangpi area is 2613 ± 177 Ma with $Sr_i \sim 0.7020 \pm 0.0044$ and is thus the oldest dyke activity in the eastern Indian craton and possibly in the entire peninsular India, suggesting earliest stabilization event.
- Trace, REE, Sr, Nd and Oxygen isotopic data of these dykes indicate that at 2.6 Ga the nearly primitive mantle below the eastern Indian Craton was metasomatised by the fluid ($\pm$ silicate melt) coming out from the subducting early crust resulting in LILE and LREE enriched, Nb and $\delta^{18}O$ depleted, variable ε_{Nd} and low Sr_i bearing EMI type mantle. Magmatic blobs of this metasomatised mantle were subsequently emplaced at deeper levels of the granitic crust which possibly originated from the same thermal pulse.

Acknowledgements

This paper forms a part of the Ph.D. thesis of AR under the "Dr. K S Krishnan" fellowship of the Department of Atomic Energy, Govt. of India. The authors thank Prof. H C Jain, BARC, Mumbai for continuous encouragement. Valuable suggestions, given by Dr. K L Ramakumar, BARC, Mumbai, during mass-spectrometric analyses are gratefully acknowledged. A R acknowledges Mr. B Mukhopadhyay, GSI, CHQ, Geodata for help during preparation of the geological map. The authors are particularly grateful to Dr. A R Basu, Dr. N Srimal and an anonymous reviewer for their critical comments that helped to improve the manuscript. This paper is our humble tribute to late Prof. A K Saha who inspired us to undertake the isotope studies of mafic-ultramafic rocks from eastern Indian craton.

References

Ahmad T and Tarney J 1991 Geochemistry and petrogenesis of Garhwal volcanics: implication for evolution of the north Indian lithosphere; *Precamb. Res.* **50** 69–88

Allegre C J 1997 Limitation between mass exchange between the upper and lower mantle: the evolving convection regime of the earth; *Earth Planet. Sci. Lett.* **150** 1–6

Arndt N T 1983 Role of thin komatiite rich oceanic crust in the Archean plat-tectonics process; *Geology* **11** 372–375

Balaram V, Ramesh S L and Anjaiah K V 1996 New trace element and REE data in thirteen GSF reference samples by ICP-MS; *Geostand Newslett.* **20** 71–78

Bennett V C, Nutman A P and McCulloch M T 1993 Nd-isotopic evidence for transient, highly depleted mantle reservoir in the early history of the earth; *Earth Planet. Sci. Lett.* **119** 299–317

Bickle M J and Eriksson K A 1982 Heat loss from the earth: A constraint on Archean tectonics from the relationship between geothermal gradient and the rate of plate production; *Phils. Trans. Royal Soc. (London)* **305** 225–247

Blusztajn J and Shimizu N 1993 The trace element variation in clinopyroxenes from spinel peridotite xenoliths from Southwest Poland; *Chem. Geol.* **111** 227–243

Bose M K and Goles G G 1970 Chemical petrology of the ultramafic minor intrusions of Singbhum, Bihar; *Proc. Sec. Symp. upper mantle project, Hyderabad* 305–326

Bowring S A, King J E, Housh T B, Isachsen C E and Podosek F A 1989 Neodymium and lead isotope evidence for enriched early Archaean crust in North America; *Nature* **340** 222–225

Chase C G and Patchett P J 1988 Stored mafic/ultramafic crust and early Archaean mantle depletion; *Earth Planet. Sci. Lett.* **91** 66–73

Demeny A, Vennemann T W, Hegner E, Ahijado A, Casillas R, Nagy G, Homonnay Z, Gutierrez M and Szabo C S 2004 H, O, Sr, Nd and Pb isotopic evidence for recycled oceanic crust in the Transitional Volcanic Group of Fuerteventura, Canary Islands, Spain; *Chem. Geol.* **205** 37–54

De Paolo D J and Wasserburg G J 1979 Sm-Nd age of Stillwater complex and the mantle evolution curve for neodymium; *Geochim. Cosmochim. Acta.* **43** 999–1008

De Paolo D J 1981 Nd isotopes in the Colorado front range and crust mantle evolution in the Proterozoic; *Nature* **291** 193–196

Devaraju T C (1995) Dyke swarms of peninsular India; *Geol. Soc. India Mem.* **33** 451p

Dupre B, Chauvel C and Arndt N T 1984 Pb and Nd isotopic study of two Archaean komatiitic flows from Alexo, Ontario; *Geochim. Cosmochim. Acta.* **48** 1965–1972

Eiler J M, Farley K A, Valley J W, Hofmann A W and Stolper E M 1996 Oxygen isotope constraints on the sources of Hawaiian volcanism; *Earth Planet. Sci. Lett.* **144** 453–468

Faure G 1992 *Isotope Geology*; (John Wiley and Sons.) 589p

Fletcher I R, Rosman K J R, Williams I R, Hickman A H and Baxter J L 1984 Sm-Nd geochronology of greenstone belts in the Yilgarn block, Western Australia; *Precamb. Res.* **26** 333–361

Galan G, Pin C and Duthon J L 1996 Sr-Nd isotopic record of multi-stage interaction between mantle derived magmas and crustal components in a collision context–the ultramafic–granitoid association from Vivero (Hercynian belt, NW Spain); *Chem. Geol.* **131** 67–91

Galer S J G and Goldstein S L 1991 Early mantle differentiation and its thermal consequences; *Geochim. Cosmochim. Acta.* **55** 227–239

Hall A 1996 *Igneous Petrology* (London: Longman Publication) 551p

Halliday A N, Lee D, Tommasini S, Davis G R, Paslick C R, Fitton J G and James D E 1995 Incompatible trace elements in OIB and MORB and source enrichment in the sub-oceanic mantle; *Earth Planet. Sci. Lett.* **133** 379–395

Halls H C 1982 The importance and potential of mafic dyke swarms in studies of geodynamic processes; *Geoscience Canada* **9** 145–154

Halls H C 1987 Dyke swarms and continental rifting: some concluding remarks; In: Mafic dyke swarms; Halls H C, Fahrig W H (eds) *Geol. Soc. Canada (Spl. Paper)* **34** 137–146

Hamilton P J, O'Nions R K, Bridgewater D and Nutman A 1983 Sm-Nd studies of Archaean metasediments and metavolcanics from west Greenland and their implications for the earths early history; *Earth Planet. Sci. Lett.* **62** 263–272

Harmon R S and Hoefs J 1995 Oxygen isotope heterogeneity of the mantle deduced from global ^{18}O systematics of basalt from different geotectonic setting; *Contrib. Mineral. Petrol.* **120** 95–114

Hawkesworth C J, Rogers N W, Calsteren P W C V and Menzies M A 1984 Mantle enrichment processes; *Nature* **311** 311–335

Hegner E, Kroner A and Hoffman A W 1984 Age and isotope geochemistry of Archaean Pongola and Ushuswana suites in Swaziland, South Africa: a case for crustal contamination of mantle derived magmas; *Earth Planet. Sci. Lett.* **70** 267–279

Hofmann A W 1997 Mantle geochemistry: the message from oceanic volcanism; *Nature* **385** 219–229

Huang X, Ziwei B and De Paolo D J 1986 Sm-Nd isotope study of early Archaean rocks, Qianan, Hebei province, China; *Geochim. Cosmochim. Acta.* **50** 625–631

Ikramuddin M and Stueber A M 1976 Rb-Sr ages of Precambrian dolerites and alkaline dykes, southeast Mysore state, India; *Lithos* **9** 235–241

Jacobsen S B and Wassarburg G J 1984 Sm-Nd evolution of chondrite and achondrite–II; *Earth Planet. Sci. Lett.* **67** 137–150

Jahn B, Wu F, Lo C H and Tasi C H 1999 Crust–mantle interaction induced by deep subduction of the continental crust: geochemical and Sr-Nd isotopic evidence from post-collisional mafic-ultramafic intrusions of the northern Dabie complex, central Chaina; *Chem. Geol.* **157** 119–146

Keppler H 1996 Constraint from partitioning experiments on the composition of subducted-zone fluids; *Nature* **380** 237–240

Kroner A and Layer P W 1992 Crust formation and plate motion in the early Archaean; *Science* **256** 1405–1411

Kyser T K 1986 Stable isotope variation in the mantle. In: Stable isotope in High temperature geological processes; Valley J W, Taylor Jr H P and O'Neil J R (eds) *Rev. Mineral.* **16**. *Mineral. Soc. Am.*, Washington DC, USA. pp. 141–164

Lahaye Y, Arndt N, Byerly G, Chauval C, Fourcade S and Gruau G 1995 The influence of alteration on the trace element and Nd-isotopic composition of komatiites; *Chem. Geol.* **126** 43–64

Loomis T P 1972 Diapiric emplacement of the Ronad high temperature ultramafic intrusion, Southern Spain; *Bull. Geol. Soc. America* **83** 2475–2496

Ludwig K R 1988 ISOPLOT: A plotting and regression program for radiogenic isotopic data; *U.S. Geol. Surv., Open-file Rep.* 91–445

MacGregor D and Basu A R 1979 Petrogenesis of the Mount Albert ultramafic massif, Quebec: summary; *Bull. Geol. Soc. America* **90** 898–900

Mallik A K and Sarkar A 1994 Geochronology and geochemistry of mafic dykes from the Precambrians of Keonjhar, Orissa; *Ind. Min.* **48** 13–24

Mattey D, Lowry D and Macpherson C 1994 Oxygen isotope composition of mantle peridotite; *Earth Planet. Sci. Lett.* **128** 231–241

McCulloch M T 1993 The role of subducted slabs in an evolving earth; *Earth Planet. Sci. Lett.* **115** 89–100

McCulloch M T and Bennett V C 1994 Progressive growth of the earth's continental crust and depleted mantle: Geochemical constrains; *Geochim. Cosmochim. Acta.* **58** 4717–4738

McDonough W F and Sun S S 1995 The composition of the earth; *Chem Geol.* **120** 223–253

McKenzie D 1995 The source regions of ocean island basalts; *J. Petrol.* **36** 133–159

McKenzie D and O'Nion R K 1983 Mantle reservoirs and ocean island basalt; *Nature* **301** 229–231

Meen J K, Eggler D H and Ayers J C 1989 Experimental evidence for a very low solubility of rare earth elements in CO_2-rich fluids at mantle condition; *Nature* **340** 301–303

Moorbath S, Taylor P N and Jones P N 1986 Dating the oldest terrestrial rocks–fact and fiction; *Chem. Geol.* **57** 63–86

Muehlenbachs K, Anderson A T and Sigvaldason G E 1974 Low $\delta^{18}O$ basalts from Iceland; *Geochim. Cosmochim. Acta.* **38** 577–588

Naqvi S M and Rogers J J M 1987 *Precambrian geology of India* (Oxford: Clarendon)

Nielsen R 1998 Partition coefficients for fertile mantle. http://www.earthref.org/GERM/data/kd/F-mantle-d.htm.

Nielsen S G, Barker J A and Krogstad E J 2002 Petrogenesis of an early Archaean (3.4 Ga) norite dyke, Isua, West Greenlang: evidence for early Archaean crustal recycling; *Precamb. Res.* **188** 133–148

Nisbet E G and Fowler C M R 1983 Model of Archean plate tectonics; *Geology* **11** 376–379

Polat A, Kerrich R and Casey J F 1997 Geochemistry of Quarternary basalts erupted along the east Anatolian and Dead Sea fault Zones of southern Turkey: implication for mantle source; *Lithos* **40** 55–68

Ramakumar K L, Aggarwal S K, Kavimandan V D, Raman V A, Khodade P S, Jain H C and Mathews C K 1980 Separation and purification of Magnesium, Lead and Neodymium from dissolver solution of irradiated fuel; *Separation Science and Technology* **15(7)** 1471–1481

Roy A, Sarkar A, Bhattacharaya S K, Ozaki H and Ebihara M 1997 Rare earth element geochemistry of selected mafic–ultramafic units from Singhbhum Craton: implications to source heterogeneity; *J. Geol. Soc. India* **50** 717–726

Rudnick R L 1995 Making continental crust; *Nature* **378** 571–574

Saha A K, Sankaran A V and Bhattacharya T K 1973 Geochemistry of newer dolerite suite intrusions within the Singhbhum granite – a preliminary study; *J. Geol. Soc. India* **14** 329–346

Saha A K 1994 Crustal evolution of Singhbhum North Orissa, Eastern India; *Geol. Soc. India* 305p

Sarkar A, Sarkar G, Paul D K , Mitra N D 1990 Precambrian geochronology of the central Indian shield; *Geol. Surv. India Spl. Pub.* **28** 453–482

Sarkar A, Roy A, Ghatak G S and Bhattacharya S K 1996 Strontium isotope study of Krol-Tal carbonates: implication to the strontium isotope flux of Himalayan rivers; *India J. Geol.* **68** 255–262

Sarkar A 1997 Geochronology of Proterozoic mafic dykes from the Bundelkhand craton, central India. In: *Procds Int conf on Isotopes in the solar system*, J N Goswami, S Sahjipal and P Chakrabarty (eds) *Phys. Res. Lab. India* 98–99

Sarkar A and Mallik A K 1995 Geochronology and geochemistry of precambrian mafic dykes from Kolar gold

field, Karnataka. In: Dyke swarms of peninsular India; T C Devaraju (ed) *Geol. Soc. India Mem.* **33** 451p

Sarkar S N and Saha A K 1977 The present status of the Precambrian stratigraphy, tectonics and geochronology of Singhbhum-Keonjhar-Mayurbhnj region, eastern India; *India J. Earth. Sci. S Roy vol.* 37–65

Sharma M, Basu A R and Ray S L 1994 Sm-Nd isotopic and geochemical study of the Archaean Tonalite-Amphibolite association from the eastern Indian craton; *Contrib. Min. Petrol.* **117** 45–55

Sharp Z D 1990 A laser based micro analytical method for the *in situ* determination of oxygen isotope ratios of silicates and oxides; *Geochim. Cosmochim. Acta.* **54** 1353–1357

Smith T E, Thirlwall M F and Macpherson C M 1996 Trace element and Isotope geochemistry of the volcanic rocks of Bequia, Grenadine Islands, Lesser Antilles Arc: a study of subduction enrichment and intracrustal contamination; *J. Petrol.* **37** 117–143

Spandler C, Hermann J, Arculus R and Mavrogenes J 2004 Geochemical heterogeneity and element mobility in deeply subducted oceanic crust; insights from high-pressure mafic rocks from New Caledonia; *Chem. Geol.* **206** 21–42

Taylor S R and McLennan S M 1985 *The continental crust: its composition and evolution*; (Oxford: Blackwell) 312p

Todland M, Jarvis I and Jarvis K E 1992 An assessment of dissolution techniques for the analysis of geological samples by plasma spectroscopy; *Chem. Geol.* **95** 35–62

Toyoda K, Horiuchi H, and Tokonami M 1994 Dupal anomaly of Brazilian carbonatites: Geochemical correlation with hotspots in the south atlantic and implication for the mantle source; *Earth Planet. Sci. Lett.* **126** 315–331

Weaver B L 1991 The origin of ocean island basalt end-member compositions: trace elements and isotopic constraints; *Earth Planet. Sci. Lett.* **104** 381–397

Widom E and Farquhar J 2003 Oxygen isotope signatures in oilivines from Sao Miguel (Azores) basalts: implications for crustal and mantle processes; *Chem. Geol.* **193** 237–255

Zhang H F, Menzies M A, Mattey D P, Hinton R W and Gurney J J 2001 Petrology, mineralogy and geochemistry of oxide minerals in polymictic xenoliths from the Bultfontein kimberlites, South Affrica: implication for low bulk-rock oxygen isotopic ratios; *Contrib. Mineral. Petrol.* **141** 367–379

Zindler A and Hart S 1986 Chemical Geodynamics; *Ann. Rev. Earth. Planet. Sci.* **14** 493–571

Zindler A and Jagoutz E 1988 Mantle cryptology; *Geochim. Cosmochim. Acta.* **52** 319–333